A COMPARATIVE STUDY OF DIGITAL IMC AND RST REGULATORS APPLIED ON A WIND TURBINE

Andreea Pintea[1], Dumitru Popescu[2]

Lucrarea de față prezintă un studiu comparativ realizat cu ajutorul a doi algoritmi de reglare extrem de cunoscuți, proiectați pentru controlul unei turbine eoliene ce funcționează în regimul de încărcare totală. Tehnicile uzuale de control în acest regim se bazează pe varierea unghiului de calare al palelor cu menținerea constantă a cuplului generatorului. Aceasta este şi abordarea aleasă pentru acest studiu. Scopul lucrării este acela de a demonstra eficacitatea algoritmilor în reglarea puterii electrice prin aplicarea lor pe un model simplificat al unei turbine eoliene. Rezultatele obținute vor fi analizate şi prezentate prin intermediul simulărilor.

This paper presents a comparative study of two well known regulation algorithms designed for a horizontal variable wind speed turbine functioning in the above rated wind speed regime. Typical control in this working regime uses pitch regulation to maintain constant the turbine's rotor speed while the generator toque is held constant. This will be also the approach chosen for this study. The goal of the paper is to demonstrate the efficiency of the two algorithms in controlling the electrical output power by means of applying them on a simplified model of a wind turbine. The obtained results will be analyzed and presented through a few simulations.

Keywords: turbine, renewable, robustness, IMC, RST

1. Introduction

The challenging advantages offered by the use of renewable energies determined an increase of the interest in finding robust methods for controlling wind turbines. The power produced through wind turbines is influenced by a few environmental factors such as the speed of the wind, its direction and also its intensity. In the same time, a wind turbine can be struck by lightning, seriously affected by excessive wind, strain, stress and even fire. The working environment is therefore dynamic and complex. This is why, the control strategy employed is very important and it becomes essential when it comes to optimizing the extracted

[1] PhD student, Dept. of Automatic Control and Computer Science, POLITEHNICA University Bucharest, Romania, e-mail: andreea.pintea@gmail.com
[2] Prof., Dept. of Automatic Control and Computer Science, POLITEHNICA University Bucharest, Romania, e-mail: popescu_upb@yahoo.com

power, reducing of costs, improving logistics, increasing the produced amount of energy and also protect wind turbine's components.

Today's wind turbines employ different control methods and strategies to achieve these goals. Rotors with adjustable blades are often used to provide better control of the turbine power. The actuators that rotate the blades to modify their incidence with the wind direction must be fast, in order to provide good power regulation in the presence of gusts and turbulence [1]. The research carried out for controlling wind turbines lead to different types of controllers and control strategies. One can find a comparative study in [2] that analyzed a PI controller, a full state feedback controller and a fuzzy controller respectively, in order to regulate the produced electrical power and to minimize the load fatigue in the turbine components in the above rated wind speed region. In [3], on the other hand, a multi-model LQG approach is debated, while in [4] the same authors propose a LPV group of controllers designed to ensure the stability of the studied turbine, H_2 and H_∞ stability and robustness for all the functioning areas.

Although such techniques offer good performances, apparently most of the commercial systems are still implemented using multiple single input single output loops [5]. Simpler algorithms provide more practical solutions and are more appropriate in industrial applications due to the fact that they are easier to be implemented on microcontrollers. This paper proposes a comparison of the performances obtained with two very familiar algorithms, based on an Internal Model Controller (IMC) and RST digital controllers. These methods are characterized by simplicity and flexibility in designing. Also they have proven to offer good results in tracking and regulation, in the same time ensuring the robustness and the stability of the system.

2. Turbine architecture description

2.1 Working regimes

Variable speed wind turbines have three main regions of operation (Fig. 1): *a) First Partial Load Area (I), b) Second Partial Load Area (II)* and *c) Full Load Area (III)*.

The first zone comprises wind speeds that vary up to approximately *4m/s*. It is considered that bellow this value, the turbines consume much more energy that they manage to produce and in consequence they are not productive, therefore a turbine is started once wind surpasses this value of the wind speed. Therefore, a solution is to maintain the turbine turned off and to permanently monitor the weather conditions in order to determine whether the turbine should start producing energy or not. Normally wind turbines start functioning when wind speeds reach 5m/s.

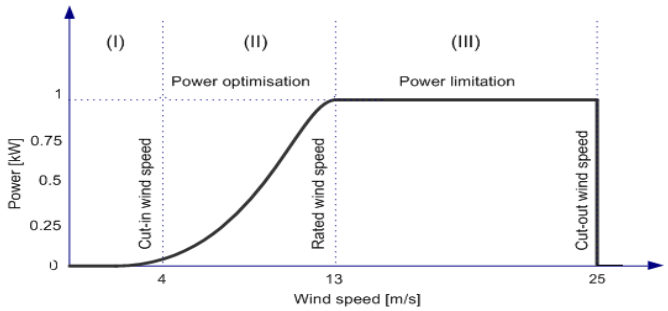

Fig. 1 Working regimes of a wind turbine

The second region is the operational mode in which the wind speeds grow enough to start producing energy; the goal changes to capturing the maximum amount of power from the air. In this area, one faces important aerodynamic losses that stop the turbine from reaching the theoretical power from the wind. Power optimization refers to finding an appropriate command to ensure the maximum allowed power extraction for a given speed of the wind.

The third region occurs above the so called "*rated wind speed*", which is the wind speed above which the maximum power peak is produced. This maximal value is defined by the nominal electric power allowed by the generator. This area corresponds to high wind speed values (over 25m/s) and to the most important mechanical solicitations of the system. The control objectives on the full area are based on the idea that the control system has to limit the output power value to the nominal value of the generator [6]. The most appealing control technique used in the Full Load zone called "*pitch control*", acts on the blades of the rotor, and it adjust them towards the feathered position, providing an effective and precise control of the output power by accelerating or decelerating the turbine's rotor. Both of the proposed algorithms use the pitch control and are designed for this regime.

2.2 Wind turbine mathematical modeling

Many mathematical ways to model wind turbines can be found in the literature. Depending on the control goal, the resulting models can be simple or complex. The reader can find different wind turbine models summarized in [6-7] and [8], each model type being calculated according to the turbine type and the control objectives. Although simple models may not characterize thoroughly the dynamic behavior of the entire wind turbine, much can be learnt from them [12]. As a plus, they offer a general image of the phenomena that happens inside a wind turbine and also of its behavior in different environmental conditions. The model used in this paper is a simplified model. The regulation goal was to maintain a constant electrical voltage, produced by the turbine, and this can be expressed in

terms of constant angular velocity of the turbine rotor. In consequence, we have eliminated the aspects that would have complicated the study.

Because wind turbines are complex systems, their modeling becomes easier if decomposed into sub-systems: namely an aerodynamic, mechanical, electric and pitch actuator (Fig. 2).

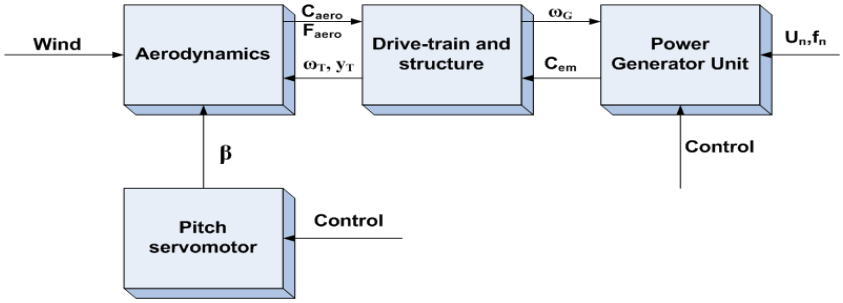

Fig. 2 Wind turbine sub-components

The aerodynamic subsystem converts the wind energy into useful mechanical energy. The aerodynamic torque C_{aero} (Fig. 2) is responsible for the rotational movement of the rotor, while the thrust force F_{aero} creates a pressure on the rotor that determines the horizontal movement of the tower that sustains the nacelle. This thrust force F_{aero} and the aerodynamic torque C_{aero} are expressed in terms of non-dimensional thrust and power coefficients, C_a and C_p respectively.

$$C_{aero} = \frac{1}{2} \cdot \rho \cdot \pi \cdot R^2 \cdot C_P(\lambda, \beta) \cdot \frac{v^3}{\omega_T} \tag{1}$$

$$F_{aero} = \frac{1}{2} \cdot \rho \cdot \pi \cdot R^2 \cdot C_a(\lambda, \beta) \cdot v^2 \tag{2}$$

with $C_p(\lambda, \beta) = c_1 \cdot (\frac{c_2}{\lambda_i} - c_3 \cdot \beta - c_4) \cdot e^{\frac{-c_5}{\lambda_i}} + c_6 \cdot \lambda$, $\frac{1}{\lambda_i} = \frac{1}{\lambda + 0.08 \cdot \beta} - \frac{0.035}{\beta^3 + 1}$ and the coefficients c_1 to c_6 being $c_1 = 0.5176$, $c_2 = 116$, $c_3 = 0.4$, $c_4 = 5$, $c_5 = 21$ and $c_6 = 0.0068$. C_a was calculated with the following expression

$$C_a(\lambda, \beta) = (0.000018851 \cdot \beta + 0.000077364) \cdot \lambda^3 + (-0.00082131 \cdot \beta - 0.0052121) \cdot \lambda^2 + (-0.0024011 \cdot \beta + 0.1595) \cdot \lambda + 0.12105 \cdot \beta - 0.25697.$$

The mechanical system comprising the rotor, the drive-train and the support structure of the nacelle, was modeled as a simplified two mass model (Fig. 3) with a flexible ax. The two masses correspond to the large turbine rotor inertia Jt, comprising the blades and hub, and the small inertia J_g representing the generator. The turbine's rotor movement is described by the following mechanical equation

$$J_t \cdot \dot{\omega}_T = C_{aero} - T_s \tag{3}$$

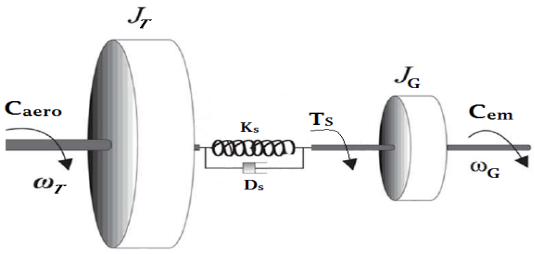

Fig. 3 The two mass model concept

In the above equation, J_t is the rotor inertia, ω_T represents the angular speed of the rotor, C_{aero} is the aero-dynamical torque and T_s is the reaction torque that appears in the drive shaft system.

The drive train's dynamics are expressed through the relation

$$T_s = K_s \cdot \gamma + D_s \cdot \dot{\gamma} \tag{4}$$

where γ is the torsion of the drive train $\gamma = \theta_T - \theta_g$.

The tower bending under the wind pressure is modeled by

$$M_T \cdot \ddot{z} = F_{aero} - D_T \cdot \dot{z} - K_T \cdot z \tag{5}$$

where z is the displacement of the nacelle in the direction perpendicular to the rotor disc. The turbine's mass is given by M_T, the damping factor by D_T and also by a spring constant K_T.

We have neglected the dynamics of the generator as they are much faster than the dynamics of the shaft when modeling the pitch control. In consequence, the equation that models the generator's motion is

$$J_g \cdot \ddot{\theta}_g = T_m - C_{em}$$

where J_g is the generator inertia, $\ddot{\theta}_g$ is the angular acceleration of the generator rotor, T_m is a mechanical torque that is driving the generator's rotor and C_{em} is the electrical torque developed by the generator (it includes losses) [9].

In order to simplify more, one imposed that all blades should move synchronously, the technique is well known as "*collective pitch"*. The blade servo is modeled as a first order system with T_{bs} as a time constant

$$T_{bs} \cdot \dot{\beta} + \beta = \beta_r \tag{6}$$

After gathering the expressions (1)-(6), we have obtained the input-output transfer functions of the model. At this point, the obtained model is highly nonlinear due to the expressions of the aerodynamic torque and of the thrust force respectively. After linearization around an operating point defined by (point S_{op} = ($\omega_{T\ op}$, β_{op}, v_{op}) = (*4rad/s, 0º, 17m/s*)) and switching to the Laplace complex domain, the model results in the following form

$$A \cdot \Delta\psi = B \cdot \beta_{ref} + C \cdot \Delta v \tag{7}$$

where A, B and C are polynomials in complex variable s (Laplace domain) and in which, the angular position of the rotor ψ, was chosen as the output of the system, the reference $\Delta\beta_{ref}$ as the control signal, while the disturbances Δv were modeled as a sudden increase of the speed of the wind and a step input was used to model them. In conclusion, we consider the system functioning around a nominal operating point, and we try to regulate the produced electrical power when a step disturbance acts upon the system. The regulator will have to maintain the electric power constant by means of controlling the turbine's angular speed.
The closed loop transfer functions with respect to wind speed change and reference signal respectively result as

$$H_p = \frac{\Delta\psi(s)}{\Delta\beta(s)} = \frac{B}{A} = \frac{213\cdot s^2 - 2.4\cdot s + 9400}{42.84\cdot s^5 + 148.5\cdot s^4 + 366.6\cdot s^3 + 814\cdot s^2 + 679.9\cdot s + 723.8} \tag{8}$$

$$H_v = \frac{\Delta\psi(s)}{\Delta v(s)} = \frac{C}{A} = \frac{2.016\cdot s^3 + 5.501\cdot s^2 + 9.84\cdot s + 21.72}{42.84\cdot s^5 + 148.5\cdot s^4 + 366.6\cdot s^3 + 814\cdot s^2 + 679.9\cdot s + 723.8} \tag{9}$$

The open loop response at a step input is depicted in Fig. 4 below. As it can be observed, the step response of the system presents a significant overshot and an oscillatory aspect.

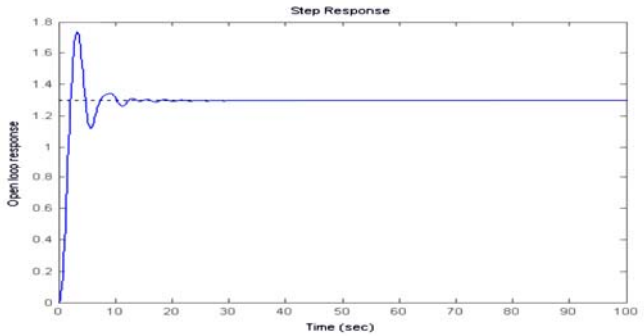

Fig. 4 The step response of the system.

The numeric values of the turbine's parameters that were used to compute the mathematical model presented above, and also in the simulations, are given in the Annex at the end of the paper.

3. Controllers design

3.1 The design of the digital RST regulator

The RST controller (Fig. 5) is a structure with two degrees of freedom. Its main advantage is that allows the designer to specify the desired performances independently with reference trajectory tracking and with regulation.

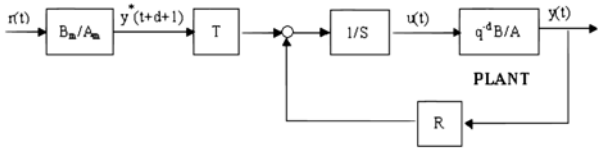

Fig.5 The general representation of a system controlled with an RST controller

In this picture the *R* and *S* blocks determine the regulation dynamics, while *T* will ensure the tracking behavior with respect to the change of the reference signal *r(t)*. Another block can be added to the system, that is defined by two polynomials *Am* and *Bm*, and that represents a trajectory generator. These polynomials are imposed by the designer according to the desired shape of the reference and in the same time with the tracking dynamics. The *R*, *S* and *T* blocks can all be written in a polynomial form, expressed by the following group of equations:

$$\begin{aligned} R(q^{-1}) &= r_0 + r_1 \cdot q^{-1} + ... + r_{nr} \cdot q^{-nr} \\ S(q^{-1}) &= s_0 + s_1 \cdot q^{-1} + ... + s_{ns} \cdot q^{-ns} \\ T(q^{-1}) &= t_0 + t_1 \cdot q^{-1} + ... + t_{nt} \cdot q^{-nt} \end{aligned} \tag{9}$$

The *R* and *S* polynomials define the closed loop regulation and will be determined first, by a matrix calculus given by

$$P(q^{-1}) = A(q^{-1}) \cdot S(q^{-1}) + B(q^{-1}) \cdot R(q^{-1}) \tag{10}$$

where *P* represents the desired closed loop polynomial of the system.

For the calculation of *T*, one must ensure a unitary static gain between the generated trajectory and the output of the system. In the end, the RST command signal results in the form:

$u(k) = \frac{T(q^{-1})}{S(q^{-1})} \cdot r(k) - \frac{R(q^{-1})}{S(q^{-1})} \cdot y(k)$, where *r(k)* is the discrete reference and *y(k)* represents the output of the system. By analyzing the poles and zeros of the system, one observes that it contains three unstable zeros. The most appropriate approach for computing the command is based on the factorization of the numerator of the system's transfer function. Namely, if one defines the $H_p = B(q^{-1})/A(q^{-1})$, where *B* contains the unstable zeros, the proposed method implies writing *B* as:

$B(q^{-1}) = q^{-1} \cdot B^*(q^{-1})$, with $B^*(q^{-1}) = B^{*+}(q^{-1}) \cdot B^{*-}(q^{-1})$ and where, B^{*+} contains all the stable zeros, and B^{*-} contains all the unstable zeros of the system. If one wants to eliminate the potential steady state error, an integrator on the direct path is needed/ Therefore *S* should be written as

$$S(q^{-1}) = B^{*+}(q^{-1}) \cdot (1 - q^{-1}) \cdot S'(q^{-1}) \tag{11}$$

The equation (10) becomes

$$A(q^{-1})\cdot B^{*+}(q^{-1})\cdot(1-q^{-1})\cdot S'(q^{-1})+q^{-1}\cdot B^{*+}(q^{-1})\cdot B^{*-}(q^{-1})\cdot R(q^{-1})=P(q^{-1})$$

By solving this matrix equation, one finds the polynomials S' and R, and consequently S and R. To find the T polynomial, one has to specify the desired tracking behavior. The closed loop transfer function of the system becomes:

$$H_{CL}(q^{-1})=\frac{q^{(-1)}B^{*-}(q^{-1})\cdot T(q^{-1})}{P(q^{-1})} \tag{12}$$

T is computed as to obtain a unitary value of the response in the permanent regime

$$T(q^{-1})=\frac{P(1)}{B(1)} \tag{13}$$

Also, to improve the tracking dynamics the trajectory generator was chosen in the form

$$\frac{Bm(q^{-1})}{Am(q^{-1})}=\frac{0.027\cdot q^{-1}+0.024\cdot q^{-2}}{1-1.58\cdot q^{-1}+0.63\cdot q^{-2}} \tag{14}$$

3.2 The design of the digital internal model controller

The Internal Model Control (IMC) strategy relies on the *Internal Model Principle* which states that control can be achieved only if the control system encapsulates a representation of the process to be controlled [10], [11]. In particular, if the control scheme has been developed on the exact model of the process, then perfect control is theoretically possible. In practice, however, process model mismatch is always present. The process model might not be invertible and the system is often affected by unknown disturbances.

The design of the discrete IMC controller (Fig. 6) implies knowing the zeros and poles of the system given by writing (8) in the poles-zeros representation.

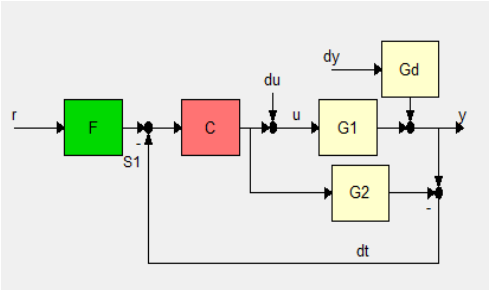

Fig. 6 The IMC control technique

The steps to compute the IMC controller are

- The poles of the model become the zeros of the controller;

- One keeps the zeros of the process model that have a positive real part and that are contained in the unit circle and
- The inverse of the zeros of the process model that have a positive real part and that are not contained in the unit circle.
- One adds a pole in the origin for each zero of the process model that has a negative real part.
- The gain of the controller is chosen such as:

  $C(1) * G_2(1) = 1$;

  The method also indicates choosing a filter to handle the modeling errors

$$F(z) = \frac{(1-\alpha)\cdot z}{z-\alpha}, \ 0<\alpha<1.$$

This filter's effect on the system response shows an increased smoothness and also a reduction of the controller's sensitivity to the modeling errors [12]. The structure and the parameters of the filter should be determined such that an optimal compromise between performance and robustness is reached. To simplify the design task one fixes the filter structure and searches over a small number of filter parameters (usually just one) to obtain the desired robustness characteristics. In our case, adjusting α is equivalent to adjusting the speed of the closed loop response. For non minimum phase systems, α becomes the dominant closed loop time constant when it is made large enough. Therefore, it slows down the system but it makes it more robust. Simulations done for the current system showed that just one filter is not enough. As a consequence we added a second one of the same form. Below we provide the transfer functions of the two filters:

$$F_1(z) = \frac{(1-0.5)\cdot z}{z-0.5} \qquad F_2(z) = \frac{(1-0.1)\cdot z}{z-0.9}$$

4. Results comparison

The simulations of the system controlled with the two proposed regulators were made using the MATLAB software. We have studied the shape of the response of the system to a step input, simultaneously considering the perturbation also a sudden variation of the speed of the wind at a given moment in time. It was observed that both controllers manage to track the imposed reference and to reject the applied disturbance.

The time rise of the system with the RST controller has a value of 3.77s. This value has been compared with the time rise of another RST controller computed for the same system through the poles placement method. The results of this method can be seen in [6]. Therefore the performances obtained with the two digital RST controllers are similar.

The step response of the system controlled with the RST controller can be seen in Fig. 8 (without perturbation) and Fig 9 (with step disturbance) while, the

response with the IMC controller is represented in Fig. 10. From Fig. 8, one can observe that the system tracks the imposed reference and that the overshot was nearly eliminated. The steady state error is zero due to the presence of the integrator on the direct path. The RST also eliminated the oscillations that were present in the open loop response.

In Fig. 9 a disturbance of 10% of the steady state value of the system's response was considered. The controller manages to reject it and to provide the required performances.

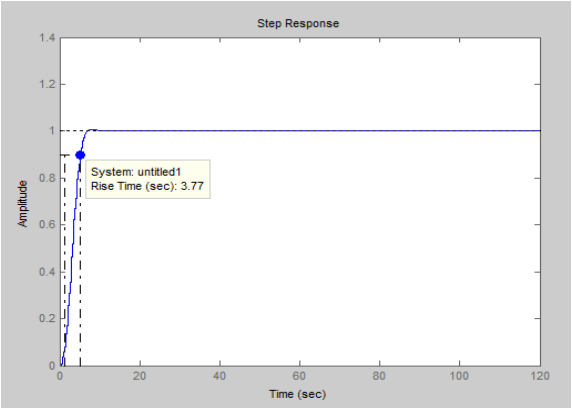

Fig 8. Response time of the system controlled with the RST

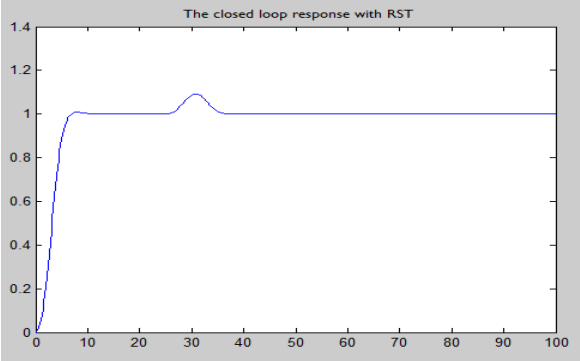

Fig 9. Closed loop response of the system with RST controller

What can be observed from the figures above is the fact that the IMC controller does not eliminate the oscillations very fast. Nevertheless, such oscillations do not have dangerous values and therefore additional corrections can be made to completely eliminate them. These disturbances come from the disturbing signal and they tend to be slightly amplified in the system with the IMC controller, due to the fact that the closed loop system does not contain an open loop pole to remedy this behavior. The RST controller on the other hand, provides a more accurate answer with respect to rejection disturbance.

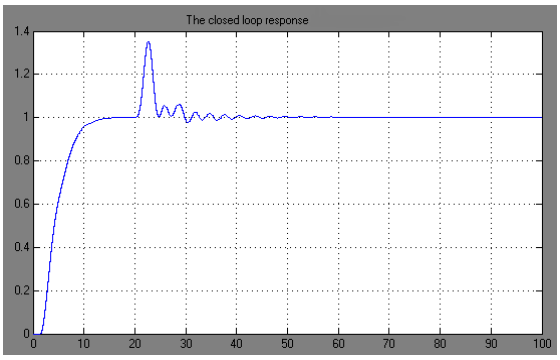

Fig10. The closed loop response of the system with IMC controller

5. Conclusions

The paper presented a comparison study made upon two digital algorithms, namely the RST and IMC controllers applied on a variable speed wind turbine. Such controllers present the advantage of being simple to design, to offer good performances and to be widely used in the industrial applications.

The study was done for the above rated wind speeds and in this regime, the difficulties in wind turbine control involve both the necessity of maintaining the output of the generator at a value which must correspond to maximization of captured energy. Nevertheless, the two studied approaches have shown good results in both tracking and disturbance rejection. Still, the internal model controller, in its classical design method, provides certain inflexibility. This disadvantage reflects in the response of the closed loop system that is inferior to the one offered by the RST controller.

A N N E X

The numerical values of the turbine parameters

Symbol	Physical meaning	Numerical value
J_t	Turbine inertia	$5.1 * 10^6$ Kg * m^2
M_T	Tower and nacelle mass	$2.1* 10^5$ kg
K_s	Drive shaft stiffness coefficient	$9.4 * 10^5$ Kg* m^2/s^2
D_s	Drive shaft damping coefficient	$1.1 * 10^4$ Kg* m^2/s
K_T	Tower stiffness coefficient	$9.4 * 10^5$ N/m
D_T	Tower damping coefficient	$1.1 * 10^4$ Ns/m

R E F E R E N C E S

[1]. *A.D. Wright, L.J. Fingersh*, "Advanced Control Design for wind turbines – Part I: Control Design, Implementation and initial Tests", Technical Report, NREL/TP -500042437, March 2008

[2]. *M. Jelavic, I. Petrovic*, "Design of a Wind Turbine pitch controller for loads and fatigue reduction", Electrical Engineering Institute, Proceedings of the European Wind Energy Conference & Exhibition – EWEC, Milan, Italy, 2007.

[3]. *F. Lescher, P.Borne, J.-Y. Zhao,* "Commande LQG d'une turbine éolienne a vitesse variable", Sciences et Technologies de l'automatique, e-STA, Volume 2, No.4, 2005.

[4]. *F. Lescher, J. Zhao, P. Borne, "*Switching LPV controllers for a variable speed pitch regulated wind turbine", Int. J. of Computers, Communication and Control, vol. 1, pages 73-84, 2006.

[5]. *C. Lupu , C. Petrescu, A. Ticlea, C. Dimon, A. Udrea, B. Irimia*, "Multi-model system with nonlinear compensator blocks", UPB Scientific Bulletin, Series C: Electrical Engineering, 70 (4), pp. 97-114, 2008.

[6]. *A. Pintea, P. Borne, D. Popescu,* "Robust control for wind power systems", Proceedings for the 18th Mediterranean Conference on Control and Automation, June 23-25, Marrakech, Morocco, 2010.

[7]. *I. Munteanu, E. Ceanga,* "Optimal control of Wind Energy Systems, Towards a global approach", Springer, 2007.

[8]. *J.F. Manwell, J.G. McGowan, A.L.Rogers*, "Wind energy explained-Theory, Design, and Application", Wiley and Sons, 2002.

[9]. *F.A. Vanegas, M. Zamacona*, "Robust control solution for a wind turbine – A simulation study", International Master's Thesis in Information Technologies, Halmstad Univeristy, February 2008.

[10]. *D. E. Rivera, M. Morari, S. Skogestad*, "Internal Model Control 4 PID Controller Design", Ind. Eng. Chem. Process Des. Dev. 25, 252, 1986.

[11]. C. *Lupu , C. Petrescu, A. Ticlea, C. Dimon, A. Udrea, B. Irimia*, "Design procedure for inverse model command: Control method for nonlinear processes", UPB Scientific Bulletin, Series C: Electrical Engineering, 70 (3), pp. 87-100, 2008.

[12]. *J.M. Flaus*, La régulation industrielle, régulateurs prédictifs et flous, Hermes, pages 116-130, 1994.